

# Single Site Electronic Spectroscopy of Magnesium Isobacteriochlorin in *n*-Octane Matrixes at 7 K

Amarnauth Singh, Wen-Ying Huang, Peter Scheiner, and Lawrence W. Johnson\*

Department of Chemistry, York College, and The Graduate Center of The City University of New York, Jamaica, New York 11451

Received: October 5, 2005

The high resolution, single site emission and absorption spectra of magnesium isobacteriochlorin (MgiBC) in *n*-octane matrixes at 7 K are reported. Its emission and Q and Soret band absorption regions have been investigated. The vibrational frequencies of the ground and the lowest energy  $\pi\pi^*$  singlet excited states were determined from luminescence and excitation spectra, respectively. The emission from MgiBC at 7 K seems to be entirely fluorescence. The luminescence and Q<sub>y</sub> region spectra of the complex are similar, having intense, narrow origin bands followed by relatively weak, but orderly vibrational structure. The Q<sub>x</sub> region does not have a clear origin and exhibits complex vibrational structure that increases in intensity going to higher energy. In the Soret region the individual  $\pi\pi^*$  origins are clearly identifiable and some vibrational structure was also observed.

## 1. Introduction

The metalloisobacteriochlorins (MiBC; Figure 1, inset) have triggered many investigations because of their importance in biological systems,<sup>1–5</sup> their potential as photosensitizers in photodynamic therapy<sup>6</sup> and as a naturally occurring variation of the fundamental porphyrin structure.<sup>7,8</sup> An example from living systems is siroheme, an iron isobacteriochlorin complex that is the prosthetic group of sulfite and nitrite reductases; these enzymes catalyze the six-electron reductions of the sulfite ion to sulfide ion and the nitrite ion to ammonia.<sup>1–5</sup> Another biological example of the importance of MiBC is nickel(II) isobacteriochlorin, a complex being used as a model for cofactor 430, a nickel tetrapyrrole found in methylcoenzyme M reductase that catalyzes the final stages of the reduction of carbon dioxide to methane in methanogenic bacteria.<sup>9,10</sup>

The synthesis, and low- and high-resolution spectroscopic studies of the free base isobacteriochlorin (H<sub>2</sub>iBC) have been reported.<sup>11–13</sup> Detailed information on synthesis and properties of octaethylisobacteriochlorin have also been published.<sup>14–18</sup> However, the electronic spectra of metalloisobacteriochlorins have not been well elucidated. It is important to fill this void because it is these moieties that are biologically active. The particular complex of interest here is magnesium isobacteriochlorin (MgiBC). This metal ion when incorporated into porphyrins forms metallocomplexes with good luminescence properties,<sup>19–23</sup> and gave us the opportunity to look at a fluorescence spectrum from a metalloisobacteriochlorin.

Here we present the single site emission and excitation spectra of MgiBC in *n*-octane matrixes at 7 K. We set out to identify the origins of the first four  $\pi\pi^*$  singlet states, Q<sub>y</sub>, Q<sub>x</sub>, B<sub>x</sub>, B<sub>y</sub>, and their associated vibrational structure. The high-resolution fluorescence spectrum of MgiBC is also reported.

## 2. Experimental Section

The magnesium isobacteriochlorin was synthesized using a modified version of the procedure developed by Egorova et al.<sup>11</sup> MgiBC: a 25 mL two-neck flask fitted with a thermometer,

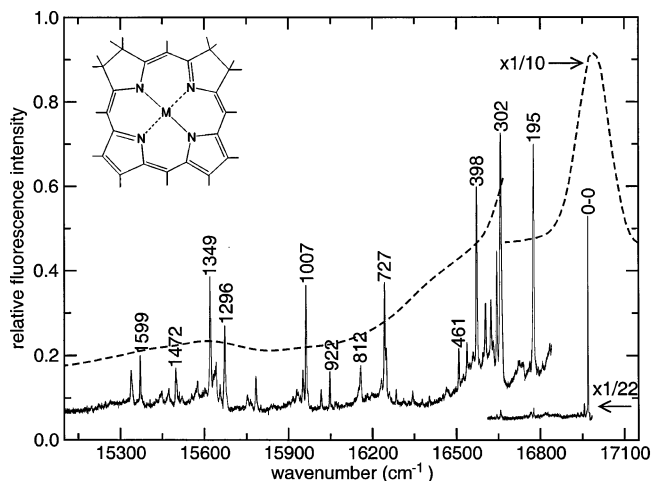


**Figure 1.** Fluorescence spectra of magnesium isobacteriochlorin in *n*-octane: Shpol'skii matrix at 7 K (—); solution at 298 K (---). The S<sub>1</sub> → S<sub>0</sub> origin band at 7 K (—) is included. The inset in the figure shows the metal isobacteriochlorin molecule.

condenser and magnetic stirrer was charged with 0.80 g (6.44 mmol) 2-(dimethylamino)pyrrole, 15 mL of 1,2-dichlorobenzene and 2.5 mL of 3 M ethylmagnesium bromide (7.5 mmol) in diethyl ether. The dark mixture was heated with stirring and samples were periodically removed and diluted with octane for UV–vis monitoring. Within 10 min (90 °C) a peak appeared at 586 nm (MgiBC:Q-band) accompanied by a smaller peak at 607 nm (magnesium chlorin:MgC). After 23 min (117 °C) the absorption ratio 586 nm:607 nm was approximately 2:1. The reaction mixture was evaporated to dryness in vacuo and the black residual solid was dissolved in CDCl<sub>3</sub>. Filtration afforded a dark red-blue solution for NMR analysis. NMR (CDCl<sub>3</sub>): 3.95 (br m, 8H, 2,3,7,8-H); 6.92 (s, 1H, 5-H); 7.53 (s, 2H, 10,20-H); 7.75 (d, *J* = 3.6 Hz, 2H, 12,18-H); 8.23 (d, *J* = 3.6 Hz, 2H, 13,17-H); 8.62 (s, 1H, 15-H). The spectrum was contaminated with MgC (35–40%). On standing at room temperature solutions of MgiBC converted to MgC. Magnesium chlorin was

also synthesized to verify the NMR identifications. MgC: 2-(Dimethylamino)pyrrole (0.80 g, 6.44 mmol), 1,2-dichlorobenzene (20 mL) and ethylmagnesium bromide (2.2 mL, 3 M in diethyl ether, 6.6 mmol) were heated (165 °C, internal temperature) with stirring in an oil bath for 5.5 h. The dark reaction mixture was diluted with CHCl<sub>3</sub> (40 mL) and filtered through Celite. Lower boiling material was removed under aspirator pressure; 1,2-dichlorobenzene was removed in vacuo. The resulting dark green solid displayed a major absorption (octane solution) at 607 nm. NMR (CDCl<sub>3</sub>): 4.68 (s, 4H, 2,3-H); 8.57 (s, 2H, 5,20-H); 8.63 (d, *J* = 4.4 Hz, 2H, 7,18-H); 8.89 (s, 2H, 12,13-H); 9.00 (d, *J* = 4.4 Hz, 2H, 8,17-H); 9.53 (s, 2H, 10,15-H).

Dilute solutions (10<sup>-6</sup> M) of MgiBC in purified *n*-octane (*n*-C<sub>8</sub>) were prepared. Room-temperature electronic absorption spectra and emission spectra were made using Perkin-Elmer (Lambda 19) UV/vis/NIR and (LS 50B) luminescence spectrometers, respectively. To make MgiBC/*n*-C<sub>8</sub> mixed crystals, dilute solutions were placed in Pyrex tubes, degassed by the freeze-thaw method, sealed, and then slowly lowered (~24 h) into liquid nitrogen. The resulting single crystals were cut under liquid nitrogen and cooled to 7 K using an Oxford Instruments CF 1204 cryostat. To make Shpol'skii matrixes, the Pyrex tubes were plunged into liquid nitrogen and then placed in the cooled helium cryostat.

High-resolution absorption spectra of the complex were made in the form of excitation spectra at liquid helium temperature. The initial scans were detected with a Jobin-Yvon THR 1500 monochromator set perpendicular to the laser excitation beam. Its wavelength was set to zero so as to monitor the total emission; two 615 nm cutoff filters were inserted in front of the entrance slit. The origin area of the S<sub>1</sub> ← S<sub>0</sub> excitation was scanned with a Lambda Physik 2001 dye laser (bandwidth 0.2 cm<sup>-1</sup>) pumped with a Lambda Physik Lextra 50 (XeCl) excimer laser. The molecule's emission, and the laser intensity, were monitored using two EMI 9203QA photomultiplier tubes in cooled housings, and a Stanford Research SR 400 photon counter. To obtain a single-site excitation spectrum, the monochromator's wavelength was then set to the S<sub>1</sub> ← S<sub>0</sub> 0-0 band and the vibronic excitation spectrum was scanned with the dye laser; the spectrum was corrected by software for the wavelength dependence of the laser's intensity. The single site excitation origin region was obtained by setting the monochromator at the strongest vibrational emission band, and then scanning the dye laser over the origin. The dyes used to cover the excitation spectra were Exciton's C540A, C500, C480, C440, QUI and Lambda Chrome's LC 3990.

High-resolution emission spectra were obtained at 7 K. The dye laser's wavelength was set at the S<sub>1</sub> ← S<sub>0</sub> 0-0 band, and the emission spectrum was scanned using the Jobin-Yvon THR 1500 monochromator in conjunction with a Stanford Research SR 510 lock-in amplifier. The single-site fluorescence origin of MgiBC was obtained by setting the laser's wavelength at the strongest vibrational excitation band and the emission spectrum was obtained by scanning the monochromator. The emission spectrum reported for MgiBC/*n*-C<sub>8</sub> at 7 K was obtained using Shpol'skii matrix because the crystal gave the same spectral features, but weak fluorescence intensity.

### 3. Results and Discussion

**3.1. Emission.** Figure 1 shows the fluorescence spectrum of MgiBC. The dashed line is the low resolution MgiBC fluorescence spectrum made with a room temperature *n*-octane solution; the solid line spectrum was made with MgiBC in an

**TABLE 1: Vibrational Frequencies Obtained from the Single Site Fluorescence Spectrum of Magnesium Isobacteriochlorin in an *n*-Octane Shpol'skii Matrix at 7 K**

$\nu_{\text{gd}}$ (cm <sup>-1</sup> ) <sup>a</sup>	<i>I</i> <sup>b</sup>	assignment <sup>c</sup>	NiOEiBC <sup>d</sup>	MgC <sup>e</sup>	H <sub>2</sub> iBC <sup>f</sup>
0	1000	0-0 (S <sub>1</sub> → S <sub>0</sub> )			
195	57	F	202		
302	60	F	299		292t, 303c
326	34	F			329c
346	23	F	346	344	344t
366	23	F	361	361	
398	47	F			392t, 405c,t
432	15	F			437
461	14	F	469		462c
720	14	F	722		717c
727	27	F	737	730	726t
812	10	F or (346 + 461) + 5	811		804t
922	9	(461 × 2)	921		927t
1007	27	F	1010	1005	997t
1019	9	F	1018	1013	1018c
1186	8	(461 + 727) - 2	1175		1170c
1296	18	F	1306		1305
1314	6	(302 + 1007) + 5	1316		
1328	11		1335	1336	1321c
1349	29	F	1347	1356	1354c
1472	9	(461 + 1007) + 4	1488		
1599	12	F or (302 + 1296) + 1	1594		1607c
1632	9	F (302 + 326 + 1007) - 3 or 1627			

<sup>a</sup> Distance of the spectral feature from the S<sub>1</sub> → S<sub>0</sub> origin (16 962 cm<sup>-1</sup>). <sup>b</sup> The S<sub>1</sub> → S<sub>0</sub> origin's intensity (*I*) was independently assigned a value of 1000; all subsequent peaks were compared to it. <sup>c</sup> F signifies a fundamental vibration. <sup>d</sup> Vibrational frequencies obtained from infrared and resonance Raman of NiOEiBC.<sup>26</sup> <sup>e</sup> Vibrational frequencies obtained from the MgC fluorescence spectrum.<sup>25</sup> <sup>f</sup> Vibrational frequencies obtained from the fluorescence spectrum of cis (c) and trans (t) H<sub>2</sub>iBC.<sup>13</sup>

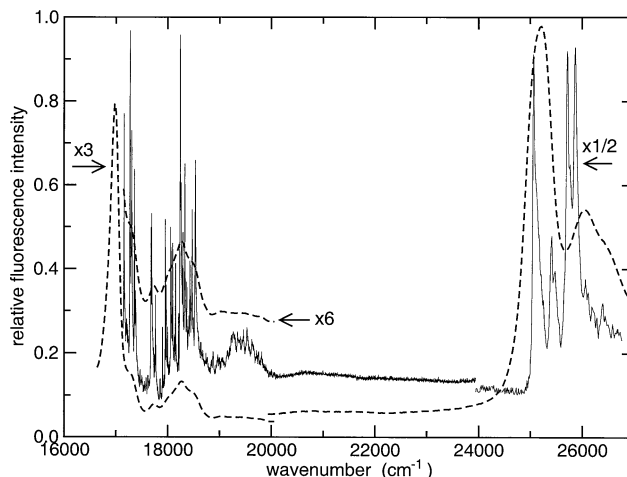


**Figure 2.** Excitation spectra of magnesium isobacteriochlorin in *n*-octane: crystal at 7 K (—); solution at 298 K (---). Both the Q and Soret regions are shown.

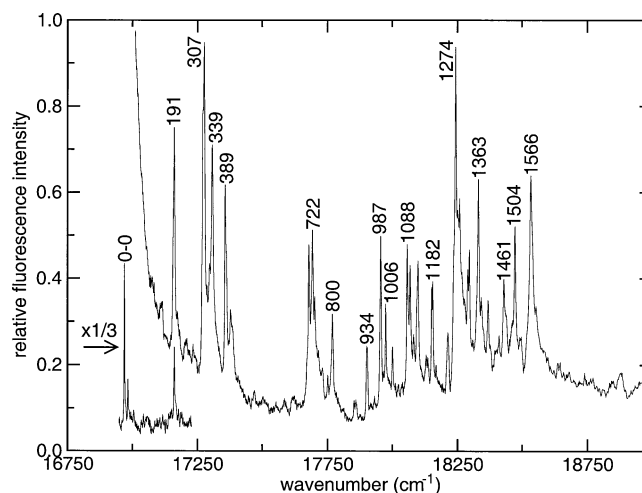
*n*-octane matrix at 7 K. The S<sub>1</sub> → S<sub>0</sub> origin is at 16 962 cm<sup>-1</sup>; the full width at half-maximum (fwhm) of the MgiBC singlet 0-0 band is 1.1 cm<sup>-1</sup>. The vibrational peak positions are summarized in Table 1. This table includes each peak's distance, in cm<sup>-1</sup>, and intensity relative to the origin; 0-0 was arbitrarily assigned an intensity value of 1000. Tentative assignments of the vibrational peaks are included in Table 1 and are compared with vibrations observed in the single site spectra of magnesium chlorin (MgC),<sup>25</sup> and free base isobacteriochlorin (H<sub>2</sub>iBC),<sup>13</sup> and with the infrared and resonance Raman spectra of Ni(II) octaethylisobacteriochlorin (NiOEiBC).<sup>26</sup>

**TABLE 2: Vibrational Frequencies Obtained from the Single Site Excitation Spectrum of Magnesium Isobacteriochlorin in an *n*-Octane Crystal at 7 K**

$\nu_{\text{exc}}$ ( $\text{cm}^{-1}$ ) <sup>a</sup>	$I^b$	assignment <sup>c</sup>	MgP <sup>d</sup>	MgC <sup>e</sup>	H <sub>2</sub> iBC <sup>f</sup>
0	1000	0-0 ( $S_1 \leftarrow S_0$ )			
191	454	F	196		
307	587	F			304c,t
327	236	F		328	328c,t
339	422	F		338	341t
389	364	F			389t
410	168	F		417	405c,t
710	268	F	713	706	712c
723	290	F	724	719	723t
732	184	F		736	739t
782	61	(389 × 2) + 4	782		
800	160	F		792	799c,t
883	23	(191 + 307 + 389)			
893	24	(191 + 710) - 8	888	897	
934	106	F	937		
987	280	F	989	985	984c,t
1006	174	F	1004	1000	1006c
1032	107	F			
1088	269	F	1091		
1100	235	F			1101c
1113	127	F	1116		
1130	242	F		1127	
1161	93	F	1159	1158	
1167	89	(389 × 3)	1164		
1182	202	F			1176c
1186	208	F			
1198	80	(191 + 1006) + 1		1198	
1244	128	F		1242	1246c
1274	582	F		1267	1274c,t
1290	340	F	1289	1293	1290c
1321	229	F	1318	1318	1314c
1327	265	F			1328t
1363	371	F			
1373	186	F or (389 + 987) - 3		1371	1374t
1400	179	F	1397		
1442	127	(410 + 1032)			1445c,t
1461	215	F	1465	1456	
1504	297	F	1508		1506c
1566	374	F			1566t
1911	66	(722 + 1186) + 3			
2222	76	(1113 × 2) - 4		2218	
2381	100	(1088 + 1290) + 3			
2492	104	(1088 + 1400) + 4			
2562	106	(1274 + 1290) - 2			
2655	88	(1327 × 2) + 1			
8096	1017	0-0' ( $S_3 \leftarrow S_0$ )			
8450(354')	472	F			
8514(418')	366	F			
8751	1023	0-0'' ( $S_4 \leftarrow S_0$ )			
8910(152'')	1036	F			

<sup>a</sup> Distance of the spectral feature from the  $S_1 \leftarrow S_0$  origin (16 962  $\text{cm}^{-1}$ ). The primed numbers indicate the distance of the spectral feature from the  $S_3 \leftarrow S_0$  origin (25 058  $\text{cm}^{-1}$ ). The double-primed number indicates the distance of the spectral feature from the  $S_4 \leftarrow S_0$  origin (25 713  $\text{cm}^{-1}$ ). <sup>b,c</sup> See Table 1. <sup>d</sup> Vibrational frequencies obtained from the MgP excitation spectrum.<sup>28</sup> <sup>e</sup> Vibrational frequencies obtained from the MgC excitation spectrum.<sup>25</sup> <sup>f</sup> Vibrational frequencies obtained from the excitation spectrum of cis (c) and trans (t) H<sub>2</sub>iBC.<sup>13</sup>

As might be anticipated, there is a substantial similarity between the vibrations seen in the fluorescence spectra (Table 1) of MgiBC, MgC, and the cis and trans forms of H<sub>2</sub>iBC. However, our spectra raise a few questions about the NiOEiBC band assignments.<sup>26</sup> For example, the MgiBC fluorescence peaks at 346 and 366  $\text{cm}^{-1}$  from the  $S_1 \rightarrow S_0$  origin seem to correspond to absorptions at 346 and 361  $\text{cm}^{-1}$  in the NiOEiBC Raman spectrum, and 344 and 361  $\text{cm}^{-1}$  in the MgC fluorescence spectrum. However, this doublet in the NiOEiBC spectrum has

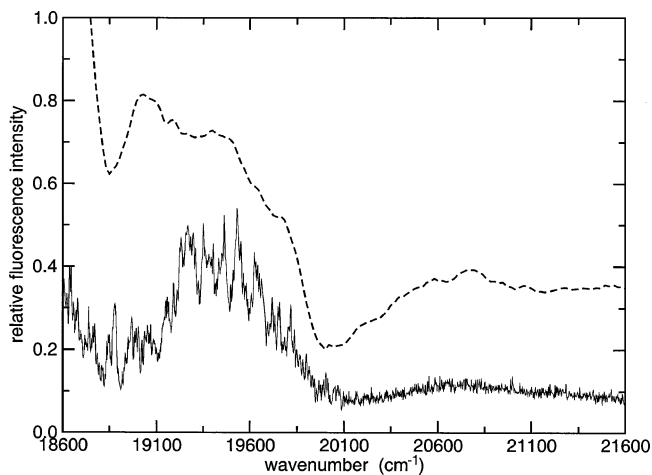
**Figure 3.** Single site excitation spectrum of magnesium isobacteriochlorin in an *n*-octane crystal at 7 K. Only the Q<sub>y</sub> region is shown; the  $S_1 \leftarrow S_0$  origin band is included.

been attributed to ethyl rotational isomers.<sup>26,27</sup> Because neither MgiBC nor MgC have peripheral ethyl groups, this assignment maybe suspicious. A similar situation arises for the MgiBC fluorescence peaks at 1007 and 1019  $\text{cm}^{-1}$  from the  $S_1 \rightarrow S_0$  origin, these seem to correspond to those at 1010 and 1018  $\text{cm}^{-1}$  in the Raman spectrum of NiOEiBC, and 1005 and 1013  $\text{cm}^{-1}$  in the fluorescence spectrum of MgC. In the Raman spectrum these were assigned as ethyl group C1-C2 modes; again this assignment seems suspect because neither MgiBC nor MgC have ethyl groups.

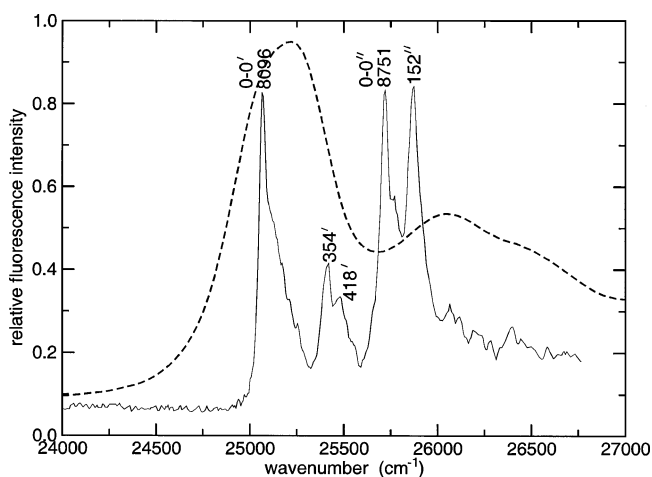
**3.2. Absorption.** The absorption spectrum of MgiBC was obtained in the form of an excitation spectrum. The full scan of the Q through B regions (16 000–27 000  $\text{cm}^{-1}$ ) is shown in Figure 2. The dashed line in each figure is the room-temperature solution excitation spectrum; the solid line excitation spectrum was made with MgiBC in an *n*-octane matrix at 7 K. The vibrational peak positions are listed in Table 2; the  $S_1 \leftarrow S_0$  origin was arbitrarily assigned an intensity value of 1000, and all other peak intensities in the spectrum were based on that assumption. The peak positions given in the table are relative to the respective  $S_1 \leftarrow S_0$  origin; tentative assignments of each vibrational peak are included and the frequencies are compared to those found in similar metal porphyrins and H<sub>2</sub>iBC.

Figure 3 shows an expanded view of the Q<sub>y</sub> region (16 750–19 000  $\text{cm}^{-1}$ ) at 7 K. The origin band of MgiBC is at 16 962  $\text{cm}^{-1}$  and has a fwhm of 1.1  $\text{cm}^{-1}$ . The Q<sub>y</sub> region consists of bands with fwhm of 5–10  $\text{cm}^{-1}$ , which form clusters of peaks overlapping with each other in going toward higher energy. Most of the vibrational frequencies of MgiBC listed in Table 2 for the Q<sub>y</sub> region are also found in the MgC/*n*-C<sub>8</sub> spectrum<sup>25</sup> at 7 K, in the MgP/*n*-C<sub>8</sub> + ethanol spectrum<sup>28</sup> at 4.2 K, and the H<sub>2</sub>iBC/*n*-C<sub>8</sub> spectra<sup>13</sup> at 7 K. The Q<sub>y</sub> region spectrum of MgiBC is essentially identical to its emission spectrum, which indicates that the geometry of the ground and first excited states are similar.

The expanded view of the Q<sub>x</sub> region (18 600–21 600  $\text{cm}^{-1}$ ) of MgiBC is shown in Figure 4. There is no clear origin band in this spectrum; however, we attempted to identify it. In Figure 4 the MgiBC spectral features have abruptly become significantly broader and more congested. This observation is consistent with the assumption that in this region the high energy vibrational fine structure of the Q<sub>y</sub> region is penetrating the Q<sub>x</sub> origin area.<sup>29</sup> We speculate that the Q<sub>x</sub> 0-0 corresponds to the highly structured, broad (fwhm ~500  $\text{cm}^{-1}$ ) band centered at



**Figure 4.** Excitation spectra of magnesium isobacteriochlorin in *n*-octane: crystal at 7 K (—); solution at 298 K (---). Only the  $Q_x$  region is shown.



**Figure 5.** Excitation spectra of magnesium isobacteriochlorin in *n*-octane: crystal at 7 K (—); solution at 298 K (---). Only the Soret region is shown. The primed numbers indicate the distance of the spectral feature from the  $S_3 \leftarrow S_0$  origin (25 058  $\text{cm}^{-1}$ ). The double-primed number indicates the distance of the spectral feature from the  $S_4 \leftarrow S_0$  origin (25 713  $\text{cm}^{-1}$ ).

about 19 400  $\text{cm}^{-1}$ , and the complex structure has been produced by the  $Q_x$  origin coupling to the background manifold of  $Q_y$  vibrational states; the magnitude of the vibronic interaction between the two states is then 500  $\text{cm}^{-1}$ .<sup>30</sup> This type of “tangled” spectral pattern has previously been observed in large organic molecules,<sup>29,30</sup> including simple porphyrins,<sup>32,33</sup> in the region of the second electronic transition and is due to the resonant coupling between the higher energy excited state and the background manifold of vibrations from the lower excited state.<sup>34,35</sup> In previous examples of resonant coupling, the spectra were highly structured but maintained the overall shape common to many  $\pi\pi^*$  transitions where there is only a minor change in geometry; that is, there is a strong origin region followed by substantially less intense spectral features due to excited-state vibrations. This overall band shape arises because the potential energy curve of the excited state is shifted with respect to that of the ground state; consequently, the origin band may have little or no oscillator strength due to a small Franck–Condon factor, whereas the transitions to excited-state vibrational levels obtain larger relative intensities due to enhanced overlap of the wave functions. We were unable to strengthen the argument for this 0–0 assignment by identifying its vibrational compo-

nents because of the low signal strength in the region above  $\sim 20\,000\ \text{cm}^{-1}$ .

The Soret region of MgiBC is shown in Figure 5. The relatively strong and sharp peaks at 25 058 and 25 713  $\text{cm}^{-1}$  are assigned as the  $B_x\ 0-0$  and  $B_y\ 0-0$  with bandwidths (fwhm) of about 110 and 125  $\text{cm}^{-1}$ , respectively. These sharp origins are each followed by vibrational bands. These states presumably have relatively long lifetimes,<sup>29</sup> based on their narrow bandwidths, and relax via a fluorescent route.

#### 4. Conclusion

We have identified the 0–0 positions of the  $Q_y$ ,  $Q_x$ ,  $B_x$  and  $B_y$  bands of MgiBC. The  $Q_x$  origin band was not observed clearly; however, it seems to be undergoing a resonant coupling with the higher vibrational levels of the  $Q_y$  band.

**Acknowledgment.** This work was supported by the National Institutes of Health (NIGMS 08153).

#### References and Notes

- (1) Murphy, M. J.; Siegel, L. M.; Kamin, H. *J. Biol. Chem.* **1973**, *248*, 251.
- (2) Murphy, M. J.; Siegel, L. M.; Kamin, H. *J. Biol. Chem.* **1973**, *248*, 2801.
- (3) Murphy, M. J.; Siegel, L. M. *J. Biol. Chem.* **1973**, *248*, 6911.
- (4) Vega, J. M.; Garrett, R. H.; Siegel, L. M. *J. Biol. Chem.* **1975**, *250*, 7980.
- (5) Murphy, M. J.; Siegel, L. M.; Tove, S. R.; Kamin, H. *Proc. Natl. Acad. Sci. U.S.A.* **1974**, *71*, 612.
- (6) Mettath, S.; Li, G.; Srikrishnan, T.; Mehta, R.; Grossman, Z. D.; Dougherty, T. J.; Pandey, R. K. *Org. Lett.* **1999**, *1*, 1961.
- (7) Ghosh, A. Quantum Chemical Studies of Molecular Structures and Potential Energy Surfaces of Porphyrins and Hemes. In *The Porphyrin Handbook*; Kadish, K. M., Smith, K. M., Guillard, R., Eds.; Academic Press: New York, 2000; Vol. 7, p 1.
- (8) Gouterman, M. Optical Spectra and Electronic Structure of Porphyrins and Related Rings. In *The Porphyrins*; Dolphin, D., Ed.; Academic Press: New York, 1978; Vol. 3, p 1.
- (9) Telsler, J.; Fann, Y.-C.; Renner, M. W.; Fajer, T.; Wang, S.; Zhang, H.; Scott, R. A.; Hoffman, B. M. *J. Am. Chem. Soc.* **1997**, *119*, 733.
- (10) Furenlid, L. R.; Renner, M. W.; Smith, K. M.; Fajer, J. *J. Am. Chem. Soc.* **1990**, *112*, 1634.
- (11) Egorova, G.D.; Solov'ev, K.N.; Shul'ga, A.M. *Zh. Obshch. Khim.* **1967**, *37*, 357.
- (12) Johnson, L. W.; Murphy, M. D.; Pope, C.; Foresti, M.; Lombardi, J. R. *J. Chem. Phys.* **1987**, *86*, 4335.
- (13) Huang, W.-Y.; Wild, U. P.; Johnson, L. W. *J. Phys. Chem.* **1992**, *96*, 6189.
- (14) Stolzenberg, A. M.; Spreer, L. O.; Holm, R. H. *J. Am. Chem. Soc.* **1980**, *102*, 364.
- (15) Montforts, F. P.; Ofner, S.; Rasseti, V.; Eschenmoser, A.; Woggon, W. D.; Jones, K.; Battersby, A. R. *Angew. Chem., Int. Ed. Engl.* **1979**, *18*, 675.
- (16) Richardson, P. F.; Chang, C. K.; Spaulding, L. D.; Fajer, J. *J. Am. Chem. Soc.* **1979**, *101*, 7736.
- (17) Richardson, P. F.; Chang, C. K.; Hanson, L. K.; Spaulding, L. D.; Fajer, J. *J. Phys. Chem.* **1979**, *83*, 3420.
- (18) Chang, C. K. *Biochemistry* **1980**, *19*, 1971.
- (19) Allison, J. B.; Becker, R. S. *J. Chem. Phys.* **1960**, *32*, 1410.
- (20) Becker, R. S.; Allison, J. B. *J. Phys. Chem.* **1963**, *67*, 2669.
- (21) Harriman, A. *J. Chem. Soc. Faraday Trans. 2* **1981**, *77*, 1281.
- (22) Noort, M.; Jansen, G.; Carters, G. W.; vander Waals, J. H. *Spectrochim. Acta* **1976**, *32A*, 1371.
- (23) Becker, R. S.; Allison, J. B. *J. Phys. Chem.* **1963**, *67*, 2675.
- (24) Adler, A. D.; Longo, F. R.; Kampas, F.; Kim, J. *J. Inorg. Nucl. Chem.* **1970**, *32*, 2443.
- (25) Singh, A.; Egbujor, R.; Huang, W. H.; Johnson, L. W. *J. Phys. Chem.* **2001**, *105*, 5778.
- (26) Melamed, D.; Sullivan, E. P.; Prendergast, K.; Strauss, S. H.; Spiro, T. G. *Inorg. Chem.* **1991**, *30*, 1308.
- (27) Li, X. Y.; Czernuszewicz, R. S.; Kincaid, J. R.; Stein, P.; Spiro, T. G. *J. Phys. Chem.* **1990**, *94*, 47.

- (28) Jansen, G.; Noort, M. *Spectrochim. Acta A* **1976**, 32, 747.
- (29) Hochstrasser, R. M. *Acc. Chem. Res.* **1968**, 1, 266.
- (30) Wessel, J.; McClure, D. S. *Mol. Cryst. Liq. Cryst.* **1980**, 58, 121.
- (31) Keegan, J. D.; Stolzenberg, A. M.; Lu, Y.-C.; Linder, R. E.; Barth, G.; Moscovitz, A.; Bunnenberg, E.; Djerassi, C. *J. Am. Chem. Soc.* **1982**, 104, 4305.
- (32) Huang, W.-Y.; Johnson, L. W. *J. Chem. Phys.* **1998**, 108, 4349.
- (33) Huang, W.-Y.; VanRiper, E.; Johnson, L. W. *Spectrochim. Acta A* **1996**, 53, 589.
- (34) Langhoff, C. A.; Robinson, G. W. *Chem. Phys.* **1974**, 6, 34.
- (35) Freed, K. F. Energy Dependence of Electronic Relaxation Processes in Polyatomic Molecules. In *Radiationless Processes in Molecules and Condensed Phases*; Topics in Applied Physics, Vol. 15; Fong, K. F., Ed.; Springer-Verlag: Berlin, Heidelberg, New York, 1976.